OPTIMIZING THE FIXED LEADING EDGE SHAPE OF A TRANSONIC WING TO SUIT THE LANDING HIGH-LIFT REQUIREMENTS*

M. Ingelman-Sundberg and L.-E. Eriksson**
The Aeronautical Research Institute of Sweden
Bromma, Sweden

Abstract

This paper describes the low speed part of a larger program at FFA for optimizing a transonic aircraft wing for the three flight phases transonic cruise at M = 0.85, manoeuvring at M = 0.5 and landing.

The low speed part was limited to droop variations for the leading edge of a basic wing with planform, thickness and twist distribution determined by transonic considerations. The sweep angle is 25°, the aspect ratio 4 and the taper ratio 0.4.

The aim of the investigation was to study if it for an attack aircraft project would be possible to avoid the complication of a leading edge flap through an optimum compromise in leading edge shape between the shape suiting transonic cruise and that suiting landing.

The experimental part was carried out in two phases. The first phase investigated experimentally the validity of shape studies made on a constant chord variable sweep research wing when applied to the real tapered and twisted wing for two droops, 1 and 2 % local chord, constant across the span. The second phase was more extensively combined with a theoretical prediction of the spanwise distribution of lift on the leading edge and the detailed pressure distribution around it and included droops spanwise decreasing outboard of 65 % span.

The gain in landing $C_{L\,max}$ for those drooped leading edges that gave acceptable transonic cruise drag characteristics was rather modest, 0.05-0.10. The improvements of the usable C_L at manoeuvre were, however, rather good. Furthermore, this investigation has given valuable knowledge about test techniques and problems and the possibilities of using computational tools for guidance.

The requirement for sufficient Reynolds number in tests of this kind is emphasized.

1. Introduction

For a light attack aircraft it was considered economically desirable if it could be possible to avoid movable leading edge flaps. A relatively extensive investigation was therefore started to find the optimum shape of a fixed leading edge for a wing with planform, twist and thickness distribution aft of the 15 % chord line given by structural and transonic requirements.(1)

For a wing without leading edge flap the problem is that the leading edge at high lift is exposed to a strong flow upwards while at low lift at high speed a slight downward flow will occur if the nose is drooped. In the first case there is the risk for separation above and in the second case below the nose. The first limits the maximum lift and the second causes drag. The latter is complicated by the fact that it occurs at high flight Mach number with risk for local supersonic regions which result in wave drag and also very likely shock induced separation.

The high lift case needs a large droop while for the high speed case the acceptable droop is limited.

To get a quick approximate idea about the effect on $C_{L\,max}$ of varied droop the low speed investigation started with experimental tests with an existing variable sweep constant chord research wing with similar wing thickness. New leading edges for that could be produced very quick by an extruding technique.(2)

Work with models with the correct wing shape started at the same time as well as back-up computational work.(3) (4) (5)

The purpose of the low speed tests was to find how large a gain in $C_{L\,max}$ a certain leading edge droop could give and of the high speed tests of how large a droop could be accepted for cruise drag reasons.

The low speed tests were performed with half model technique in the FFA low speed tunnel at $Re = 1\text{-}3.6 \cdot 10^6$, Fig. 1.

In Ref. (1) the transonic part of the investigation is reported together with some of the main results from the low speed tests.

* The investigation has been sponsored by the Swedish Defense Materiel Administration.

**The wind tunnel tests have been supervised by R. Nordvik and S. Stridsberg.

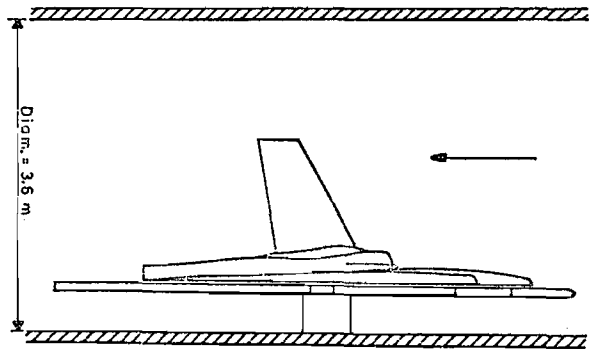

Figure 1. The FFA low speed tunnel with the half model test rig

2. The Basic Wing Geometry and Its Modifications

The basic wing, PT-100, had been designed using an inverse method aimed at a wing-body configuration with a critical Mach number of about $M = 0.85$ at $C_L = 0.2$ by designing for an upper surface maximum local Mach number of 1.2 for this case. This resulted in a wing, PT-100, with a rather large twist, almost 6^o, Fig. 2, see also Refs. (1) and (6).

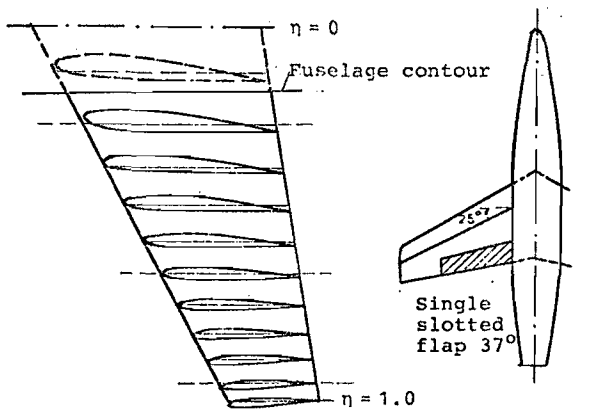

Figure 2. Geometry for the basic wing PT-100

The design method defined the vertical location of the leading edge but it could not - being a small disturbance method - yield the leading edge itself, which was designed in the following way. The leading edge radius at the root section was chosen to be 1 % and at the tip 2 % of the local chord. A number of transition curves from the leading edge circle to the main wing at 15 % chord were studied with calculation of detailed pressure distributions with a two-dimensional method for the high lift case. The curve giving the mildest pressure gradient after the suction peak was chosen, see also Fig. 8.

For the first phase of the low speed tests using the constant chord research wing, Fig. 3, with the vertical location of the leading edge drooped 1 % and 2 % of the chord, transition curves from the leading edge circle to the main wing at 15 % chord were chosen as above. The largest droop was intended to be slightly too large to be expected acceptable for the high speed case, PL-101,-102, with PL-100 corresponding to section for PT-100 at $\eta = 0.95$.

Also in the first phase, low speed models with the correct wing shape (PT-100) were made and equipped also with a leading edge drooped 1 % at the root and 2 % at the tip (PT-102).

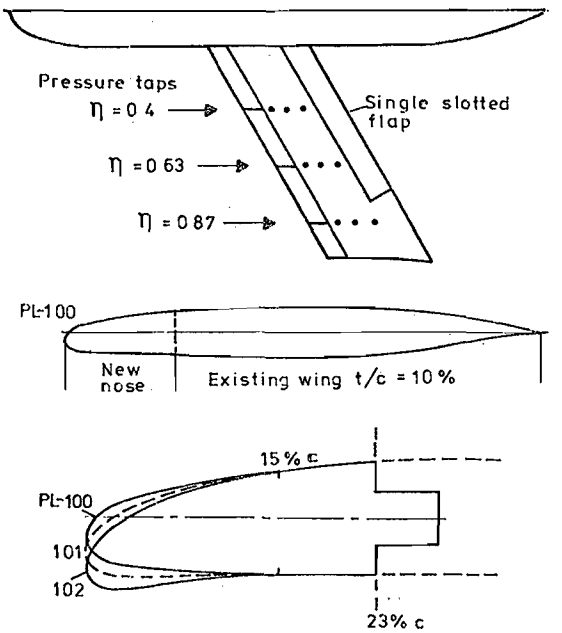

Figure 3. The constant chord research model with new leading edge parts, PL-100, 101 and 102 (streamwise chord 0.74 m)

When the first low speed tests, and also calculations, had shown that the part of the leading edge critical for $C_{L\ max}$ was at $\eta \sim 0.6$ but that the critical part at transonic cruise drag was further out, it was decided to test a droop at low speed which decreased towards the tip, the PT-104, 105 and 106. PT-105 and 106 were later high speed tested at NAE up to $Re = 18 \cdot 10^6$ and showed the expected better drag characteristics. The vertical leading edge location for all the PT-wings tested is shown in Fig. 4.

Both the constant chord wing and the correctly shaped wings were equipped with good, but not specifically optimized, single-slotted trailing edge flaps. They were sufficiently effective to make the leading edge the critical part for $C_{L\ max}$.

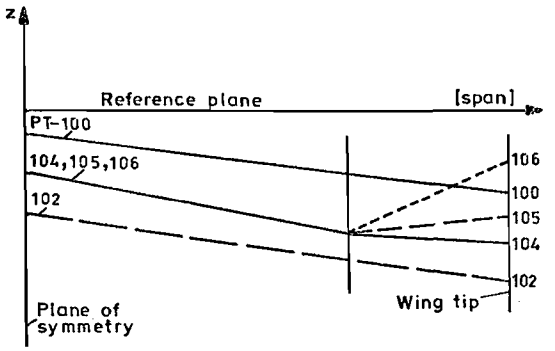

Figure 4. Vertical leading edge location along the span for all PT-configurations, shown schematically

3. Computational Methods

The theoretical tools that have been used in this work are the following:

a) A two-dimensional panel method for the calculation of pressure distributions on wing sections in subsonic flow.

b) A three-dimensional vortex lattice method for obtaining load distributions on wings in subsonic flow.

c) An approximate theory for leading edge flow at high lift making it possible to calculate the leading edge pressure distribution on a three-dimensional wing by combining the two previous methods.

d) A three-dimensional higher order panel method for the computation of pressure distributions on wings at subsonic flow.

The theory behind the panel methods and the vortex lattice method is well established and these methods are valuable tools in the design of wing geometry. The fully three-dimensional panel method is for economical reasons limited to be used as a reference method that gives the correct global flow characteristics for attached subsonic flow at high lift. It is, however, possible to utilize the fact that this flow is locally rather two-dimensional around the leading edge and thereby construct an approximate computational procedure for the leading edge pressure distribution. This procedure combines the two-dimensional panel method and the three-dimensional vortex-lattice method which both are fast and inexpensive calculational methods. The principles of the procedure are described in the following points:

1. The vortex-lattice method is used to obtain the fully three-dimensional load distribution on the wing. In this calculation, it is possible to simulate deflected trailing edge flaps.

2. A local leading edge load $C_{\ell_{L.E.}}$, Fig. 5, is calculated by integrating the load distribution obtained under point 1 in the chordwise direction from the leading edge to a specified part of the local chord, here from 0 to 10 % of the local chord. This local leading edge load varies along the span of the wing and is a measure of the strength of the two-dimensional flow around the leading edge, Fig. 6.

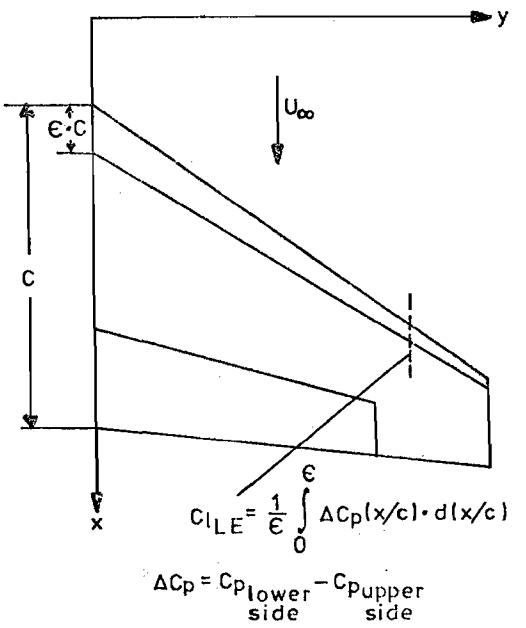

Figure 5. Definition of local leading edge load

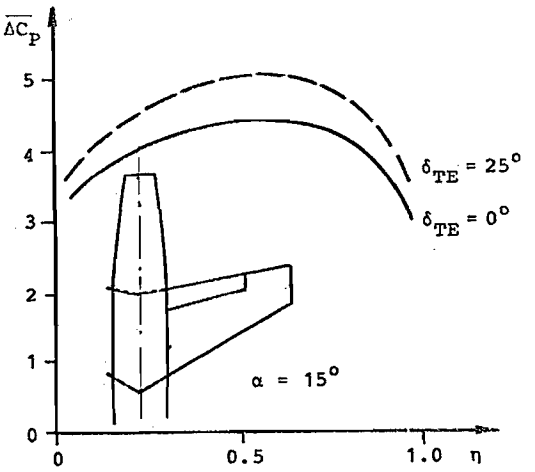

Figure 6. The leading edge load distribution over the span for PT-100 wing defined by the average $\overline{\Delta C_p}$ for x = 0 - 10 % ·C

3. To determine the pressure distribution around the leading edge at a certain station, the two-dimensional panel method is used to calculate the flow around a section at right angles to the leading edge at the station in question.

The infinite swept wing theory is then used to correct the two-dimensional results for the sweep of the leading edge. In the two-dimensional calculations, a fictitious two-dimensional angle of attack is used as a control parameter to vary the circulation around the whole section and thereby to vary the leading edge load. By a simple iterative scheme, the circulation is varied until the correct local leading edge load (as determined under point 2) is obtained. The end result is then the desired pressure distribution around the leading edge.

The approximate procedure described above has been checked against the fully three-dimensional panel method for some cases and the agreement is very good for a limited region near the leading edge, typically the first 10 percent of the local chord. For leading edge geometry modifications, the procedure therefore provides an inexpensive and rapid calculational tool to analyze the effects on the pressure distribution of a larger number of geometry variations. It has here been used to illustrate the severity of the boundary layer environment near the leading edge.

In Fig. 7 the suction peak value, $C_{p\ min}$, is used as a measure of the severity across the span in order to indicate which nose would be most prone to separate and where. A still more accurate method would be to present the pressure distribution for the individual sections in the so called canonical form, i.e. made dimensionless with the maximum local dynamic pressure. Fig. 8 shows such an example for $\eta = 0.95$ for the PT-101, 105 and 106, and that the decreased droop for PT-106, desirable for the transonic case, creates the most adverse gradient for the boundary layer.

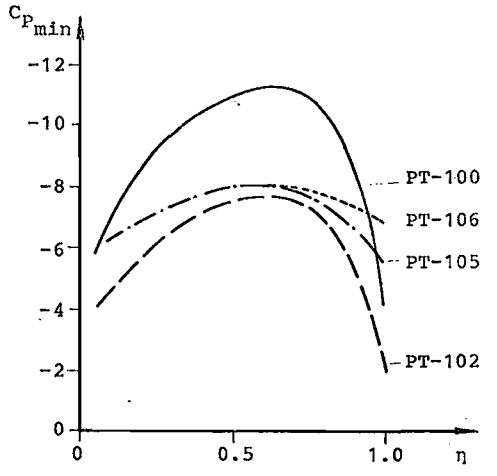

Figure 7. Calculated leading edge suction peak, $C_{p\ min}$, for the same average $\overline{\Delta C_p}$ over the spanwise location for wing PT-100 - PT-106 ($\alpha = 15^o$, $\delta_{TE} = 0$)

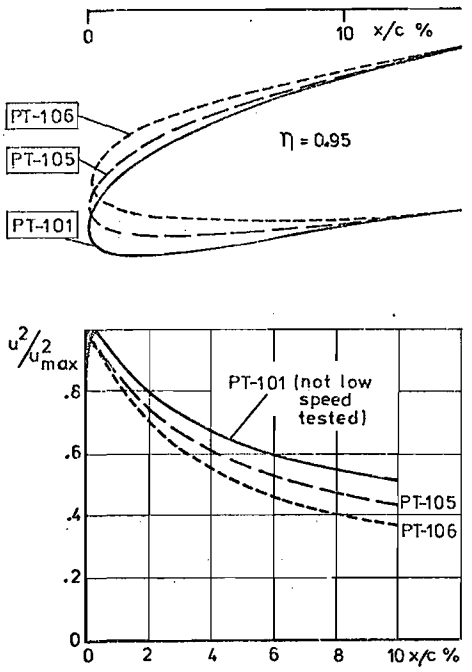

Figure 8. Canonical pressure distribution for the leading edge upper surface at $\eta = 0.95$ as illustrated by the local speed ratio u^2/u^2_{max}

4. Tests with the Constant Chord Wing Model

The tests with constant chord instead of with the correct wing planform were made because only new leading edges to the existing research model were needed and those could be produced in a short time with the extruding technique. The goal was to get a rough idea of how much a certain droop of the leading edge could mean for $C_{L\ max}$ for a wing with a thickness such that it was limited by leading edge separation.

The basic philosophy behind the test was that the separation for the real wing will start at a certain spanwise location at the leading edge. It was also assumed that a certain droop change for this section would delay the start of separation by approximately the same amount as for the constant chord wing.

The real wing differs from the research wing in two main ways, it is tapered and it is twisted. The taper causes increased local C_L towards the tip but the twist works in the opposite direction and therefore the differences to a certain extent can be said to balance each other with regard to the surroundings for the critical spanwise section.

For the high speed case the flow and separation conditions below the leading edge are important. These were therefore specially studied on the large low speed

model as a guide for the interpretation of the first high speed tests which had to be done at rather low Reynolds number. The use of transition trips for simulating a higher Re was studied.

In order to show how two-dimensional the flow around the leading edge would be the pressure distribution around it was measured in 3 spanwise sections for the PL-100 and the most drooped case, PL-102.

For the sections at $\eta = 0.40$ and 0.63 the pressure curves almost coincided but at $\eta = 0.86$ the leading edge load was slightly lower. The balance measured integrated lift gains therefore can be regarded also as a measure for the sectional gain at the location $\eta = 0.60$-.70. Here video recorded tuft studies of the stall development showed initial separation at the leading edge for the flapped case. For the non-flapped case and the highest Re the initial separation was at the trailing edge for the most drooped nose.

Effect of Reynolds Number and Transition Tripping

The limiting physical phenomenon for this type of wing both for the high lift case and the high speed case is boundary layer separation near the leading edge. In the first case it occurs above and in the second below it. Unfortunately, this is sensitive to the Re value. Especially there is the risk that the model can have a long laminar bubble type of separation when at full scale Re there would be a short laminar bubble or a fully turbulent one. It will be assumed that at full scale it will be one of the latter types both above and below the nose.

Figure 9 shows the effect of Re on $C_{L\ max}$ for the constant chord model tests.

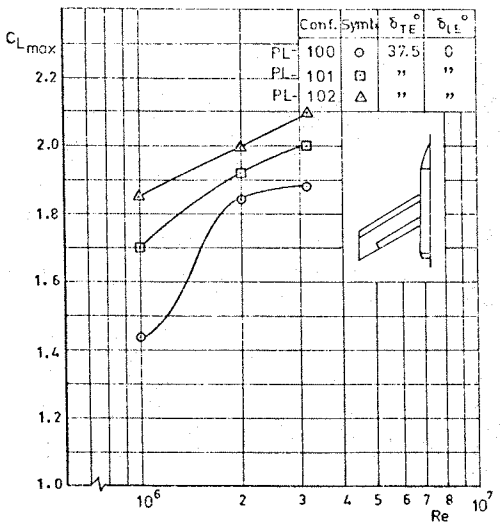

Figure 9. The gains in $C_{L\ max}$ for the constant chord model for varying Reynolds number

As the purpose of the investigation was to find the gains due to drooping it is to be observed that the influence on the $C_{L\ max}$ gain itself is so large that tests at too low Re seem meaningless.

The effect of Re on the flow below the nose is shown in Fig. 10 for PL-102 at simulated transonic cruise $C_L = 0.1$. The surface flow studies show a long bubble at Re $1 \cdot 10^6$ which changes to a very short one at $3 \cdot 10^6$.

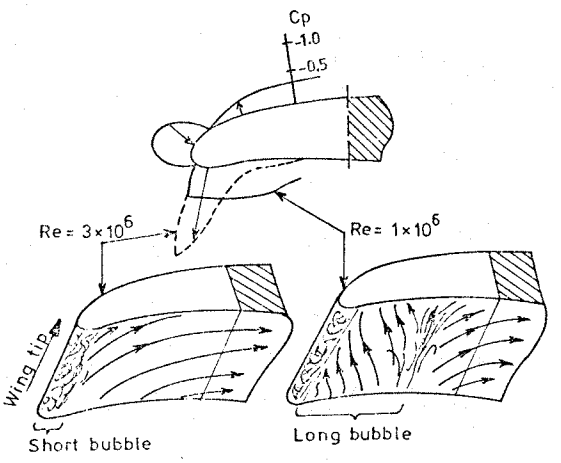

Figure 10. Reynolds number effects on the flow below the leading edge at $C_L = 0.1$ for PL-102 wing

The result for Re = $2 \cdot 10^6$ falls half way between those for Re = 1 and $3 \cdot 10^6$. The effect on the balance measured drag for this case cannot be judged due to poor balance accuracy at the low Re. If C_L is decreased below 0.1 there is, however, a marked increase in drag for the drooped PL-102 compared with PL-100, Fig. 11, and which is caused by an increased separation bubble. At $C_L = -0.1$ for PL-102 a large bubble existed even at the highest Re = $= 3 \cdot 10^6$ according to the pressure measurements.

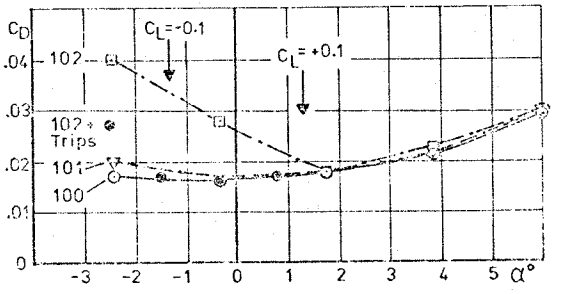

Figure 11. Drag effects due to separation below the leading edge and their elimination with transition trips (constant chord wing PL-102 at Re = $3.1 \cdot 10^6$

In order to study what would happen to the drag if the bubble disappeared at full

scale Re, transition trips were tested just forward of the separation line. At Re = 2 and $3 \cdot 10^6$ it was possible to eliminate the separation but not at Re = $1 \cdot 10^6$.

When the trip removes the separation the drag for PL-102 becomes the same as for the non-drooped PL-100. At the same time the suction peak changed from $C_p = -0.8$ to -3.9, which shows that a Reynolds number effect could very easily hide a Mach number effect at higher flight speeds.

The tests with the transition trip were carried out mainly with its use in the high speed tests in mind. However, as positioning them even for the larger low speed model turned out to be rather difficult their use on the small high speed models seemed too difficult to be acceptable.

5. Tests with Correctly Shaped Wings, the PT-Wings

The tests were performed in two separate periods, first with PT-100 and PT-102 and later with PT-104, 105 and 106. Balance measurements and flow studies with tufts and oil flow were done and also some smoke studies. For PT-102 a few pressure ports under the tip leading edge were used to check expected suction peaks at C_L corresponding to cruise. The stall development was recorded on video tape and for some cases on film.

The Flow and the Stall Development

For the basic wing PT-100 near maximum lift some flow characteristics can be mentioned.

The tuft and oil flow tests showed that there was a disturbance from the junction with the fuselage before the wing stalled. Also just before the stall there was a vertical expansion of the boundary layer wake material from the main wings upper and lower surface above the otherwise completely attached flow over the flap. None of these phenomena seemed, however, to influence the final stall. This instead spread from approximately $\eta = 0.6$-0.7 at the leading edge. Movie pictures are necessary to see it because the spread is very fast over most of the wing.

The effect of Reynolds number on PT-100 was very large between 2 and $3 \cdot 10^6$ but much less between 1 and $2 \cdot 10^6$ and almost negligible between 3 and $3.6 \cdot 10^6$, Fig. 12.

For all the wings the lift loss is very large when the final stall occurs. It is debatable if this is not inevitable for a wing which is optimized for maximum lift over the whole planform.

For the PT-106 for which the droop at the tip was changed so much in comparison with PT-100 that the leading edge was in fact slightly bent upwards the stall

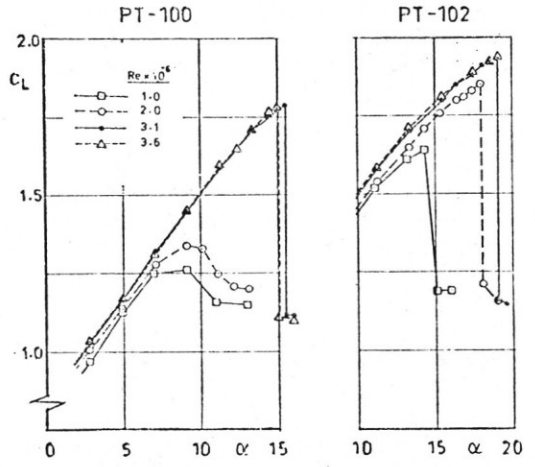

Figure 12. The difference in Re effects for PT-100 and PT-102

started at the tip and spread as fast as for the PT-100.

The flow below the leading edge at the tip and at cruise $C_L = 0.1$ which for the PT-102 showed a separation bubble even at Re = $3 \cdot 10^6$ has been changed for PT-106 indicating that the risk for suction peaks and local separation even at higher speeds would be diminished, Fig. 13.

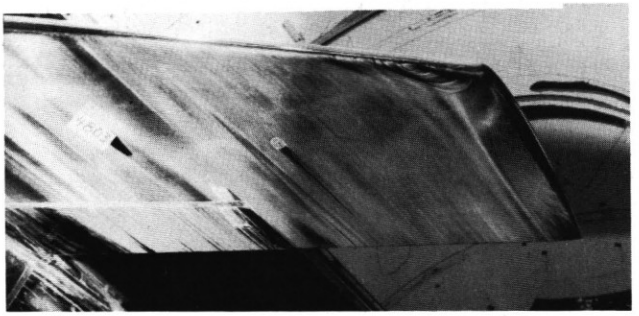

PT-102

PT-106

Figure 13. Flow under the leading edge at the tip at $C_L = 0.1$ for PT-102 and 106

The Gains in Maximum Lift

The gains in $C_{L\ max}$ for all the PT-wings are shown in Fig. 14.

First it must be observed that obtaining sufficient Reynolds number is even more important for these wings than for the constant chord model. The reason is probably the change from long bubble to short bubble separation that occurs at different Re due to different local boundary layer environment. The $C_{L\ max}$ values are valid for the flap setting of 35^{o} and small improvements of the order 0.02-0.04 have been observed by increasing the setting to 40^{o}. It is, however, assumed that this will not influence the gains from leading edge changes. A more complete flap optimization could possibly give larger improvements.

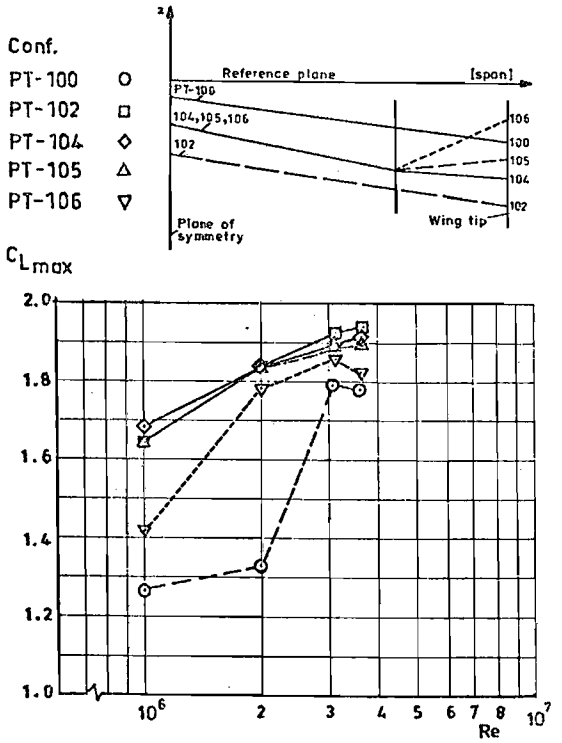

Figure 14. $C_{L\ max}$ and gains for all the PT-wings

The gains for the landing case from the transonically acceptable droop are rather modest which of course is partly owing to the fact that the basic wing PT-100 had a relatively favourable leading edge from the beginning. The decrease in $C_{L\ max}$ at the highest Re for PT-100 and PT-106 is probably due to compressibility effects as the local leading edge Mach number then is ~ 0.75.

For the manoeuvre case at M = 0.5, however, the gains are much more important. Fig. 15 shows results from the high speed test[1] where the rather large gain in usable C_L with regard to buffeting onset is visible.

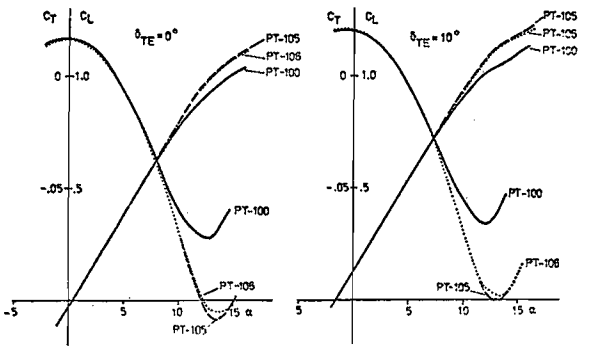

Figure 15. C_T and $C_L = f(\alpha)$ for PT-100, 105 and 106 at M = 0.5. Flap setting 0 and 10^{o}

Comparisons with Constant Chord Wing Tests and Calculations

The tests with the constant chord wing and the PT-102 made it possible to check the applicability of the inexpensive type of test.

For the PL wing with constant section all along the leading edge, 1 and 2 % droop gave $\Delta C_{L\ max}$ 0.12 and 0.24 respectively.

For PT-100 and PT-102 the stall started at the same location, $\eta = 0.65$, at the leading edge. The relative droop at $\eta = 0.65$ for PT-102 is 1.4 % which means that the gain in $C_{L\ max}$ of 0.17 would be expected. The result PT-100 to 102 was 0.16 for the same Re = 3.1.

At least for a wing with this combination of twist and taper applicability of results from tests with inexpensive constant chord models seems quite acceptable.

If the assumption is made that for a case when the leading edge radius is not changed the suction peak is a measure of the severity of the boundary layer environment and thus determines when the stall occurs the following comparisons can be interesting, see Fig. 16.

The $C_{p\ min}$ for the constant chord wings PL-100 and PL-102 are plotted versus α near stall, the highest α being 0.5^{o} below stall. Extrapolating the curves correspondingly would indicate stall at $C_{p\ min}$ = = -14.5 and -13.5 respectively. The rather small difference indicates that the assumption is not too bad.

The 2 % droop of PL-102 delays the α for $C_p = -13$ approximately 4.5 degrees. With the $dC_L/d\alpha$ for PL-100, this would correspond to a $\Delta C_{L\ max} = 0.28$, which can be compared with the experimental 0.24.

In Fig. 16 also calculated values of $C_{p\ min}$ at $\eta \sim 0.65$ (the lowest value along the span) are plotted for PT-100 and PT-102. The delay in α for the same C_p

between PT-100 and PT-102 is 3.2 degrees, which with the $dC_L/d\alpha$ for PT-100 would correspond to a $\Delta C_{L\ max} = 0.20$ to be compared with 0.16 from the tests.

If these calculations based on the $C_{p\ min}$ criterion had been carried out in advance they would thus have been able to predict the gains from the leading edge droops regarding landing $C_{L\ max}$ relatively well.

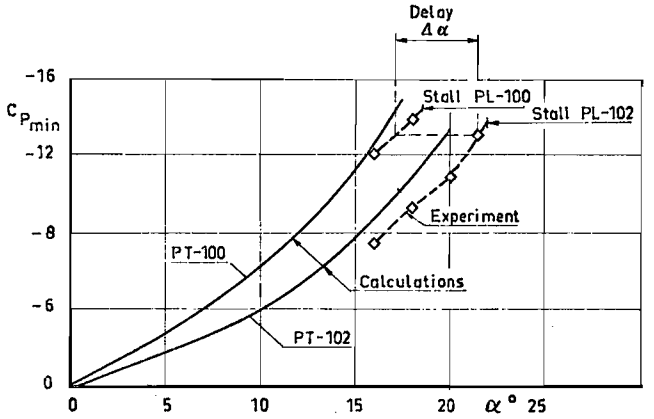

Figure 16. Experimental and calculated $C_{p\ min}$ versus α for the PL- and the PT-100 and 102 wings

Sensitivity to Leading Edge Disturbances

In connection with the tests with transition trips on PT-100 the ordinary trip, consisting of small protuberances in mylar tape 0.3 mm high, 2 mm apart, was inadvertently put on in an angle 45° across the leading edge at $\eta = 0.65$. The effect of this on $C_{L\ max}$ was surprisingly large, a $C_{L\ max}$-drop of 0.4. In the later test period with PT-104 - 106 some further tests were done, Fig. 17.

The effects shown must be considered as examples only, because no complete variation of spanwise location was done. It is thus not possible to say how large the sensitive or, for PT-104, insensitive portion of the leading edge is.

The curves are presented to show that possibly the sensitivity to disturbances has to be included in the optimization procedure besides the pure maximum lift if such relatively small irregularities as the small protuberances of the wrongly located transition trips can have so large effects.

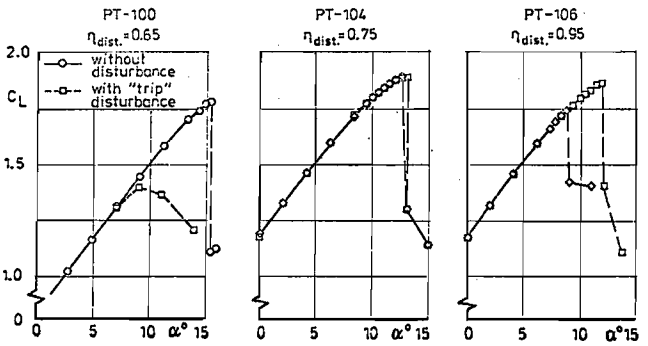

Figure 17. Examples of sensitivity to leading edge disturbances for PT-100, 104 and 106. Re = $3.1 \cdot 10^6$

Conclusions

Although the effect of the droop acceptable for transonic cruise drag on the $C_{L\ max}$ for landing was not large, the investigation has shown that in combination with tailoring the leading edge to the local spanwise needs, it can give some gains.

Computational methods used for the leading edge spanwise tailoring have been of great value. Further, more refined tailoring could give desired stall characteristics and possibly also slightly larger $C_{L\ max}$ gains.

The use of experimental leading edge studies on a simple constant chord swept wing model has shown good agreement with more complete tests on wings with taper and twist.

The necessity of sufficiently high Reynolds number for experimental leading edge optimization is shown. The risk is otherwise that the effect of a geometry variation of test Re is only to change the type of separation and that this change in any case would occur on the original shape when Re is increased to the full scale value.

References

(1) Drougge, G.: An investigation of a swept wing-body configuration with drooped leading edge at low and transonic speeds. AGARD FDP Symposium on Subsonic/Transonic Configuration Aerodynamics, Munich, May 1980.

(2) Stridsberg, S.: An investigation, using a constant chord swept wing, of possible gains in $C_{L\ max}$ with different leading edge droops designed considering transonic drag. FFA Technical Note AU-1489 (to be published).

(3) Nordvik, R.: An investigation of the high lift capabilities of the 25^{o} swept transonic wing PT-10 with and without drooped leading edges. Configurations 100 and 102. FFA Technical Note AU-1520, Part 1, 1979.

(4) Nordvik, R:: An investigation of the high lift capabilities of the 25^{o} swept transonic wing PT-10 with and without drooped leading edges. Configurations 104, 105 and 106. FFA Technical Note AU-1520, Part 2, 1979.

(5) Eriksson, L.-E.: Calculation of leading edge load and pressure distribution for swept tapered wings with deflected trailing edge flaps at low speed by a combined 3-D vortex lattice method and 2-D vortex panel method (to be published).

(6) Schmidt, W. and Hedman, S.: Recent explorations in relaxation methods for three-dimensional transonic potential flow. ICAS Paper 76-22, Ottawa, 1976.